sustainability

MDPI

Article

A Continuous-Simulation Approach for the Design and Long-Term Performance Assessment of Infiltration Basins for Sustainable Urban Water Management

Antonio Zarlenga * and Aldo Fiori

Department of Civil, Computer Science and Aeronautical Technologies, Roma Tre University, Via Vito Volterra 62, 00146 Rome, Italy; aldo.fiori@uniroma3.it

* Correspondence: antonio.zarlenga@uniroma3.it

Abstract

This study proposes a comprehensive methodology for the design and performance assessment of infiltration ponds integrated within hybrid grey–green urban drainage systems. The scope of the ponds is twofold: (i) increase infiltration of rainwater, and hence groundwater recharge, and (ii) decrease pluvial discharge downstream. The framework is applied to the Rome Technopole district, which serves as a pilot case for testing and demonstrating the procedure. Through 30-year continuous simulations performed with the EPA Storm Water Management Model and forced with a 5 min historical rainfall, the approach enables a performance-based evaluation that captures the full hydrological variability and the hydraulic performances of urban drainage systems. The methodology relies on physically based models for both the grey stormwater drainage network and the infiltration ponds, combined with a long-term simulation and functional analysis under transient conditions. The approach explicitly represents the main hydrological processes, including runoff generation, flow routing, storage dynamics, infiltration, and soil moisture variability, enabling a quantitative evaluation of peak-flow attenuation, infiltration efficiency, groundwater recharge volumes, seasonal variability, and wet–dry cycle behaviour. The latter is used to assess the long-term evolution of pond performance and its implications for maintenance activities, including clogging development and removal. Scenario analyses explore the influence of pond geometry and storage volumes, highlighting the trade-offs between hydrological efficiency, evaporation losses, and drawdown times. Beyond the specific application to the Rome Technopole developed in this study, we propose a generalizable, practitioner-oriented design procedure suited to contexts where infiltration-based solutions are desirable but regulatory guidance is fragmented. The proposed design workflow identifies critical parameters for both the hydraulic design and the operational management of infiltration ponds, enabling a statistical evaluation of their performance. The analysis of peak-flow reduction, infiltrated volumes, and the timing and frequency of wet–dry cycles provides a robust technical basis for the proper sizing, integration, and long-term assessment of infiltration ponds within urban drainage planning.

Keywords: infiltration pond; LID infrastructures; urban groundwater recharge; urban flooding; grey–green drainage systems

Academic Editor: Fernando António Leal Pacheco

Received: 18 March 2026
Revised: 18 April 2026
Accepted: 28 April 2026
Published: 2 May 2026

1. Introduction

In 2026, the metropolitan area of Rome hosts about 4.36 million inhabitants, with decades of demographic growth driving fragmented expansion toward peripheral

areas. This urbanization has progressively transformed drainage systems from natural configurations into engineered infrastructures, initially conceived for hydraulic protection and later adapted to manage increasing runoff due to soil sealing and discontinuous receiving water bodies [1]. As the city expanded, the drainage network evolved into an extensive grey infrastructure designed to collect and convey stormwater to surface waters through end-of-pipe solutions [2,3]. However, the stratification of networks built in different periods, and the limited ability of receiving water bodies—never intended to sustain current hydraulic loads—now require the adoption of innovative technologies for more effective and sustainable water-resource management [4,5].

Current stormwater control in urban environments, such as the one considered in this study, relies on a collection and conveyance system, complemented, when required, by in situ treatment units and storage structures. These storage facilities typically consist of impervious tanks sized according to district or regional regulations and designed to gradually release the stored volumes to the receiving water body. Although this approach preserves the hydraulic capacity of the receiving system, it presents several critical limitations, especially in densely urbanized contexts. Detention tanks may require large storage volumes (in Rome, they can reach hundreds of m^3/ha), resulting in a significant loss of space and land available for other urban functions. From a hydrological perspective, moreover, stored water, even when meeting quality standards suitable for potential reuse, is often discharged to ensure timely tank emptying, and therefore, the resource is seldom effectively valorized.

Low-Impact Development (LID) infrastructures, and more broadly Nature-Based Solutions (NBS), have progressively emerged as an alternative paradigm designed to overcome the limitations of conventional grey drainage systems [4,6–8]. These strategies promote water storage or controlled infiltration as an alternative to direct discharge into surface water bodies, aiming to partially restore the natural hydrological processes disrupted by extensive urban soil sealing [4,9]. A key factor contributing to the increasing adoption of LID systems is their high flexibility with a variety of possible configurations [6,10]. Importantly, LID practices are not intended to replace traditional drainage networks; rather, they are most effective when integrated into grey infrastructure systems to enhance overall hydraulic performance [4,9]. LID systems actively contribute to mitigating increased runoff volumes, attenuating peak flows and flooding risk [11,12]; beyond that, they generate a set of additional benefits such as improving urban liveability, contributing to mitigating the urban heat island effect, enhancing biodiversity, and supporting the ecological functioning of urban environments (e.g., [11,13,14]).

Some of the LID infrastructures that have been proposed over the years partially overlap with similar techniques adopted for Managed Aquifer Recharge (MAR), e.g., infiltration basins (see, e.g., [15]), but their function, due to LID systems, is as infiltration-enhancing structures that facilitate groundwater recharge [16] and support the health of soils and groundwater resources. By increasing residence times and enabling percolation through the vadose zone, they improve water quality, strengthen biogeochemical filtering processes, and foster more resilient urban hydrological regimes (e.g., [17]).

In Italy, the regulatory framework governing LID and infiltration structures is still emerging. Although some regulations address specific hydraulic or water quality aspects, a comprehensive technical guideline for designing infiltration systems is currently lacking, and this gap is also recognized at the European level within broader water-policy implementation reports, where design standards for infiltration basins remain fragmented. Although several agencies provide operational manuals [18–22], these documents vary widely in methodology, assumptions, and applicability, and no globally harmonized standard exists. Recent reviews also highlight the limited availability of uniform infiltration-basin

design protocols, despite growing international interest in green infrastructure and Nature-Based Solutions [23]. Widely adopted technical manuals typically provide practitioners with simplified design procedures intended to support routine feasibility assessments and implementation decisions, while the existing literature on LID systems is extensive, encompassing studies that examine these infrastructures from multiple perspectives with varying degrees of depth, generality, and transferability across diverse environmental and urban contexts.

Focusing on physically based methodologies, traditional design approaches for infiltration ponds are grounded in water-balance formulations and steady-state or event-based infiltration estimates (e.g., [24–27]). These deterministic schemes have been complemented by probabilistic frameworks that capture storm variability and pre-filling effects Raimondi and Becciu [28]. In parallel, numerical investigations for infiltration facilities have been developed, giving significant insight into the design of infiltration structures [29–31]. Water-quality aspects are central to the security and proper functioning of infiltration facilities and have been examined from the stormwater–groundwater interaction [32,33]. Recent advances in infiltration structures include a risk-oriented analytical framework for MAR basin design that explicitly accounts for rainfall stochasticity, subsurface heterogeneity, and groundwater-quality considerations [34]. Accordingly, residence time and vadose-zone transport processes emerge as key determinants of contamination risk, clogging propensity, and long-term operational performance—since the unsaturated zone governs storage, attenuation, and migration of infiltrating water and co-transported contaminants [35,36]. Overall, the hydrologic design of infiltration basins—and LID structures more broadly—remains an active area of debate and innovation [37]. However, the effective design of LID systems requires integrating these guidelines with a careful evaluation of multiple interconnected factors—most notably long-term maintenance needs, local rainfall regimes, and site-specific conditions—that ultimately govern their hydraulic and environmental performance [5,38,39].

This work presents the methodology adopted for the design of the drainage system of the new Rome Technopole area, with particular emphasis on the integration of NBS. The analysis specifically focuses on the *infiltration ponds* that have been incorporated into the conventional grey drainage network. The scope of the ponds here are twofold: to attenuate the flooding events, and hence decrease the discharge downstream, and to increase the infiltration of the rainwater and hence groundwater recharge, the latter minimizing the risk of contaminating the vadose zone or the underlying aquifer [34]; while the first objective can be achieved through conventional grey infrastructure (e.g., detention storage and flow regulation), the second inherently requires an infiltration-based facility.

The design workflow relies on the continuous simulation of a long rainfall record measured in Rome, enabling a performance-based evaluation that captures the full temporal variability of rainfall, runoff generation, infiltration dynamics, and system response under realistic climatic forcing; this approach overcomes some of the limitations of the approaches based on hydrological design event (see, e.g., the discussion in [40–42]). While the application presented in this study is limited to the analysis of the measured rainfall record, the method can be readily extended to synthetic rainfall fields to investigate larger return periods, as exemplified by Fiori et al. [42] for river-flood analysis. It is worth noting, however, that generating synthetic rainfall series at a high temporal resolution—such as the one used here—while fully preserving intensity–duration–frequency (IDF) relationships remains a challenging task [43]. Since our focus is on return periods on the order of a decade, the available 30-year time series is adequate for the purposes of this study.

Within this general framework, the study identifies three main aspects for evaluating the feasibility of infiltration ponds: infiltration efficiency, peak-flow reduction, and the dura-

tion of dry periods. The first is assessed as the ratio between the absolute volume infiltrated and the percentage of total runoff managed on-site; the second corresponds to the reduction in peak discharges conveyed downstream; and the third is expressed as the probability that the pond remains dry for a given period; hence, both the hydrological (preservation of runoff volumes ante and post operam) and hydraulic invariance (preservation of peak discharge) are implicitly considered here. We also assess the functional behavior of the pond by simulating wet–dry cycles and the temporal distribution of storage levels—an aspect of particular relevance for ensuring proper infrastructure maintenance, e.g., the removal of clogged layers. These metrics are essential for understanding operational reliability, resilience to sequential storm events, and susceptibility to long residence times that may influence performance and clogging. Scenario analyses are conducted to explore the hydrological implications of different pond dimensions designed in accordance with existing regulations. The analyses were carried out using the SWMM modeling framework [44], which enables the simulation of LID through simplified hydrological models and benefits from extensive technical documentation as well as strong support from a large and active user community. This choice is consistent with the objective of providing a framework that can be easily reproduced by practitioners. Potential water quality issues associated with water infiltrating through the ponds are not examined in this study, although such aspects may be relevant [34], especially in urban contexts.

While the Rome Technopole constitutes a site-specific application, the proposed workflow can be readily adopted in other design settings. Our purpose is not only to optimize the Technopole system, but also to provide a replicable, practitioner-oriented approach that can be adapted to other urban contexts, provided that local climatic forcing and site-specific hydrological and geological conditions are explicitly accounted for.

2. Study Area and System Description

The new Rome Technopole is part of an urban regeneration program in the Pietralata district, located within the Rome IV Municipality. The project area is currently characterized by open green surfaces and residual minor activities, and is enclosed within a densely urbanized context. The main development area, shown in Figure 1, includes three main buildings, their facilities, a public green space located in the western sector, and the access road system at the south-eastern boundary.

The geological and hydrogeological characteristics of the site is based on the detailed mapping provided by Vigna et al. [45], which offers one of the most comprehensive reconstructions of the subsurface setting across the Roman area. According to this study, the project site is predominantly underlain by volcanic deposits from the Alban Hills, consisting of heterogeneous pyroclastic units, ranging from unconsolidated to lithified, resting upon the deep Pliocene clay complex of the Monte Vaticano Unit. The main phreatic aquifer lies at depths greater than 15 m below ground level, ensuring no direct interaction with the planned surface infrastructures. The overlying lithoid volcanic formation exhibits good hydraulic conductivity, making it potentially favorable for infiltration-based solutions. Climatically, the area belongs to the Mediterranean regime, characterized by mild, rainy winters and hot, dry summers, with rainfall primarily concentrated in autumn and winter.

The stormwater management system designed for the Rome Technopole is organized into two main subsystems:

- W—the western subsystem ($\simeq$15,050 m^2), which drains runoff from green areas, building roof surfaces, and non-trafficable areas; water collected by this system is characterized by a low risk of contamination;

- E—the eastern subsystem (≃6850 m^2), which collects runoff from access roads and adjacent areas; since this system also handles road runoff, a pre-treatment unit is required as required by the local regulations.

The overall scheme is configured as a hybrid grey–green drainage system, where the conventional collection and conveyance network is integrated with two infiltration ponds located upstream of the receiving structures.

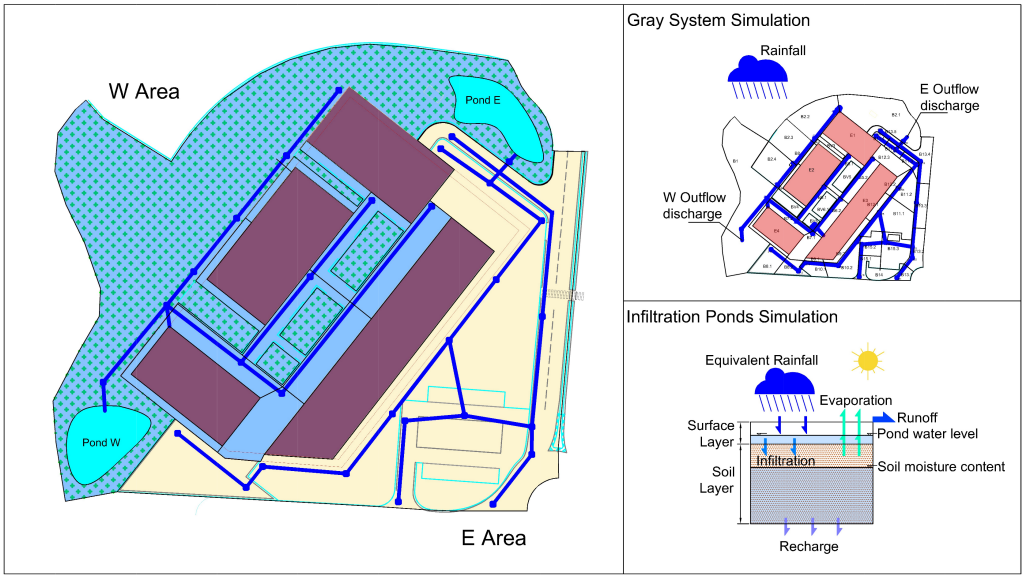

Figure 1. The main panel shows the study area, highlighting the two drainage systems serving the Eastern (yellow) and Western (blue) sectors. Top-right panel presents the grey drainage systems modeled in the first step, while bottom-right panel illustrates the operational scheme of the ponds as represented in the second modeling step.

Rainfall characterisation of the area was carried out using data from the Macao rain gauge; the dataset (53 years) allowed the derivation of the intensity–duration–Ffequency (IDF) curves through standard hydrological analyses. The design of the grey drainage network was performed using the rational method, assuming a 25-year return period for the design storm. In compliance with national regulations, particularly regarding hydraulic invariance and protection of receiving waters, the eastern subsystem includes a first-flush retention tank for runoff from traffic areas and two detention basins with volumes of 460 m^3 and 410 m^3. The retention volumes were sized using a design-storm based rainfall method consistent with the Italian hydraulic invariance approach.

The integration of infiltration ponds with the grey system was evaluated through two design scenarios:

- Scenario 1: Two compact ponds (base area 100 m^2, maximum water level 1 m) operating in parallel with the downstream detention basins, managing minor events and enhancing infiltration. The main hydraulic attenuation remains delegated to the detention structures that receive the overflow from the ponds.
- Scenario 2: Two larger ponds (base areas 460 m^2 and 420 m^2, effective depth 1 m) fully replacing the detention basins. Although this solution is hydrologically and economically more efficient, it requires a precise evaluation of drawdown times to ensure compliance with regulatory constraints.

3. Methodology

The analysis of the infiltration ponds was carried out through a 30-year continuous simulation. The rainfall time series driving the model consists of a long historical record

collected at the Roma Macao rain gauge, located close to the study area. The series has a 5 min sampling interval, a resolution fully consistent with the short response times typical of urban drainage systems and adequate for representing transient hydrological dynamics. Data were provided, upon request, by the Regional Hydrological Service. The total length of the series adequately catches the seasonal and inter-annual variability of the hydrologic response of the system and is in line with the return periods analyzed here.

Simulations have been performed using the Storm Water Management Model (SWMM) developed by the U.S. Environmental Protection Agency (US-EPA), which is a widely adopted tool for simulating drainage network hydraulics under both single-event and long-term conditions (e.g., [11,39,46–48]). The software incorporates the main hydrological models and modules for the simulations of Low-Impact Development (LID) practices. Its open-source availability and extensive scientific validation have established SWMM as a reference model for both practitioners and researchers [18,44].

In the SWMM version adopted in this study, an external inflow hydrograph cannot be directly assigned to an infiltration pond represented through the LID module. Therefore, we implemented a two-step modeling procedure. In the first phase, only the grey drainage system was simulated, with the objective of determining the total runoff discharge $Q(t)$ entering in the pond. In the second phase, this hydrograph was converted into an equivalent rainfall intensity time series, $R_{eq}(t)$, and used as input to a dedicated SWMM model developed specifically for the infiltration pond simulation. The conversion is based on a simple area scaling, and the $R_{eq}(t)$ is calculated as $R_{eq}(t) = Q(t)/A_{pond}$ with A_{pond} as the pond surface area. This transformation preserves the inflow volume exactly and the temporal pattern of the original hydrograph (i.e., peaks and timing are maintained, subject to the model time step). No additional time interpolation was introduced beyond the discretization already adopted in the simulations; Q(t) and $R_{eq}(t)$ are evaluated on the same time grid. By construction, representing a concentrated inflow (e.g., a pipe outlet) as an equivalent areal input implies a spatially uniform distribution of inflow over the pond surface. This simplification is consistent with the lumped nature of the LID representation and is expected to have a negligible impact for the small pond sizes and temporal resolution considered here. Potential limitations may arise for very large ponds or specific configurations (multiple reservoirs) not considered here. Since the analysis focuses on long-term performance metrics (volumes, seasonal patterns, wet–dry cycles), the local near-inlet hydraulics are outside the scope of the adopted lumped modeling approach. The Rome Technopole grey systems (system W and system E) representation required the definition of approximately 40 subcatchments and 35 conduits. Each subcatchment was characterized based on its geometric and hydrologic properties; infiltration was modeled using the Horton equation, with parameters previously validated in earlier studies. The conduits were described by their geometric characteristics and standard hydraulic parameters, and flow routing was simulated using the Dynamic Wave scheme. All the system setup parameters were selected using standard configurations documented in the EPA guidelines [44]. The infiltration ponds have been represented by using the LID module Bio-Retention Cell, and the ponds occupy the full subcatchments; only the surface layer and the soil layer were activated. Model parameters were defined, where possible, in accordance with the geometry of the ponds and the site's geologic characterization.

The surface layer is represented as a simple storage element whose total capacity is defined by the horizontal area of the pond (which varies across scenarios) and the vertical height of the berm (set to 1 m). This layer receives the inflow imposed as equivalent rainfall, while infiltration and evaporation are outflow fluxes activated whenever water is present in the layer. Actual evaporation is computed internally based on the potential evaporation provided as input. Runoff occurs only when the water level exceeds the

maximum storage depth of the surface layer. The infiltration rate depends on the hydraulic properties of the underlying soil layer, whereas runoff depends solely on the exceedance of the storage threshold.

The soil layer, positioned immediately below the surface layer, represents the functional core of the infiltration pond, as it governs the infiltration dynamics.

It is modeled, in this case, as a single, vertically homogeneous, effective soil layer with a depth of 4 m and hydraulic properties corresponding to a sandy loam texture. Following a commonly adopted approach in hydrological modeling within the SWMM LID module, the system does not explicitly simulate the advance of the wetting front nor the vertical post-event moisture redistribution within the soil profile; i.e., the soil hydraulic state is characterized by an average moisture content throughout the profile, and all internal fluxes are dynamically controlled by it according to the constitutive equations implemented in the SWMM LID module [18]. Although simplified, this multi-reservoir conceptualization preserves the fundamental physical behavior; nonetheless, this lumped conceptualization may lead to a less precise estimation of the infiltration rate during the earliest stages of a storm by neglecting the high initial suction of a dry surface and could potentially overestimate evaporation during prolonged dry periods by allowing moisture extraction from the entire depth. Despite these limitations, the simple model ensures very low computational demand, which is particularly advantageous for long-term (multi-decadal) simulations. Further details, together with the comprehensive mathematical formulation, can be found in [18,44].

Clogging and the associated reduction in the bottom hydraulic conductivity is not considered within our framework, while a constant conductivity was assumed for the pond bottom. This assumption reflects an operational scenario in which the infiltration pond is regularly maintained to preserve its infiltration capacity. One of the proposed analyses is specifically aimed at defining a maintenance schedule, identifying the time windows in which scraping can be operated to restore or preserve the pond-infiltration capacity.

The potential evapotranspiration (ET_0) required to quantify the system outgoing fluxes was estimated using the Hargreaves–Samani method, a widely consolidated approach in hydrology and especially suited for contexts with limited meteorological data availability, as it only requires air temperature as input [49,50]. Its applicability in data-scarce environments is further supported by several studies, including Moeletsi et al. [51]. The required air temperature and radiation time series used to implement the method were obtained from the NASA POWER database [52], which provides satellite-derived, analysis-ready meteorological and radiative datasets at hourly to monthly temporal resolutions, updated in near real time and broadly validated for agroclimatic and environmental applications. We emphasize that the specific method adopted for estimating ET_0 is not a constraint of the proposed design workflow; practitioners may implement the most appropriate formulation based on local data availability and climatic conditions.

Before presenting the analysis of the results in the next Section, it is useful to illustrate the system behavior through a simulation example covering several rainfall events. Figure 2 presents, across different panels, a portion of the time series of the main hydrological variables, which are used to illustrate the dynamics of the system during the second phase of the simulations (infiltration pond analysis). The selected window includes alternating rainfall and drying periods, and the activation and cessation of the various processes can be clearly observed. Panel A shows the fluxes occurring in the surface layer: the blue line represents the inflow entering the pond (volume per 5 min time step), while the red line depicts the runoff (volume per 5 min time step) generated when the pond exceeds its storage capacity and discharge occurs toward the outflow. Panel B displays the stored water volumes: the light-blue line represents the ratio between the water depth and its

total pond height, whereas the orange line indicates the soil saturation. Panel C illustrates the subsurface fluxes: the orange line denotes the infiltration rate (expressed per 5 min interval), while the green line represents groundwater recharge. When a rainfall event occurs (e.g., at $t \simeq 273$ h), the incoming discharge (blue line in Panel A) is conveyed into the pond, resulting in an increase in water depth (light-blue line in Panel B). The presence of water in the pond activates infiltration (orange line in Panel C). The infiltration rate is not constant: it progressively decreases as soil moisture increases, which reduces capillary forces and therefore the soil infiltration capacity. Infiltration ceases once the pond is fully emptied. If the total rainfall volume is sufficient to fill the pond completely (e.g., at $t \simeq 274.4$ h), surface runoff is activated (red line in Panel A) and continues until the pond water level falls below the elevation of the spillway. The increase in soil moisture also triggers groundwater recharge (green line in Panel C), whose magnitude is proportional to soil saturation. The decrease in water stored in the pond (e.g., between $t = 273.3$ h and $t = 274.2$ h) is governed primarily by infiltration, which in turn depends on the hydraulic conductivity of the soil material and on the soil saturation. During the pond's dry periods, the depletion of water stored in the soil (for $t > 276.4$ h) occurs; the latter is a lower process driven by both deep percolation and evapotranspiration.

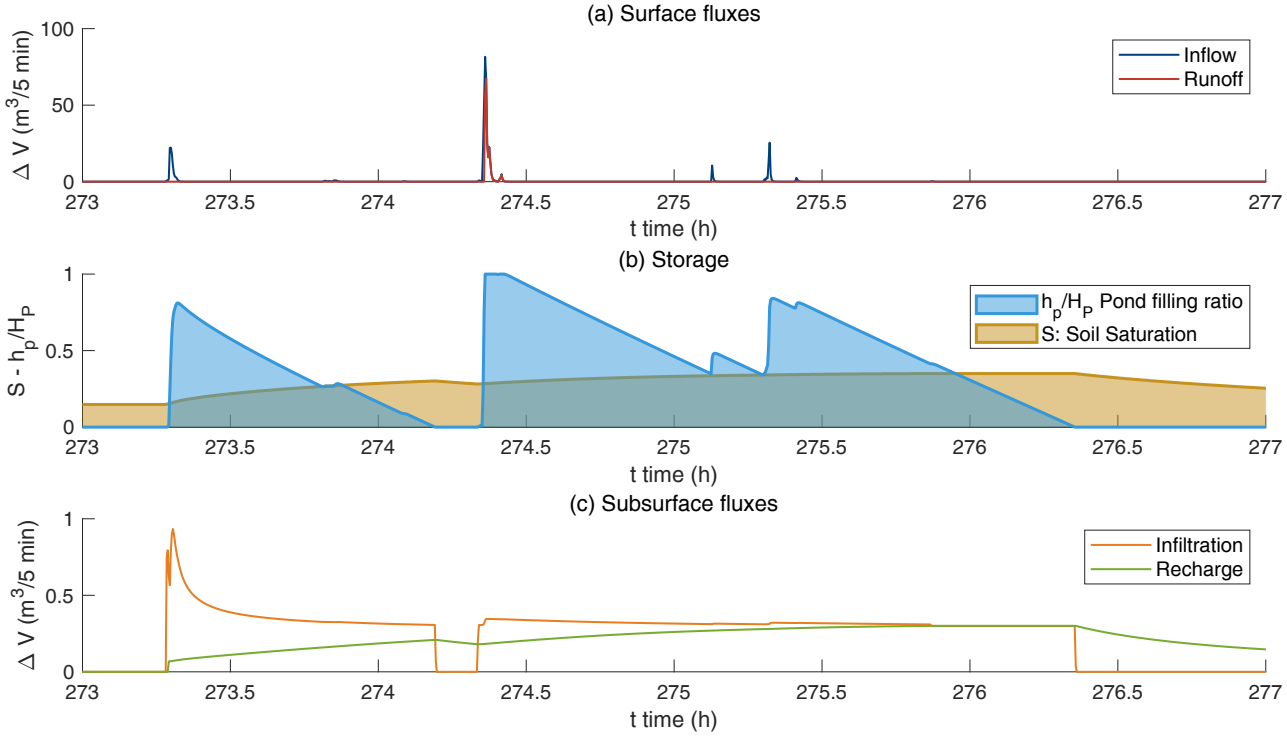

Figure 2. Panel (**a**) shows the surface-layer fluxes: the blue line represents the inflow volume to the pond, while the red line indicates the runoff discharged from the system; both are shown at a 5 min resolution. Panel (**b**) displays the water stored within the system, with the light-blue line corresponding to the relative pond water level and the orange line corresponding to the relative soil saturation. Panel (**c**) illustrates the subsurface fluxes: the orange line represents the infiltration volume, whereas the green line denotes groundwater recharge, both at a 5 min resolution.

4. Results

The discussion of the results presented below is a functional analysis of the ponds, with the aim of highlighting the key aspects that should be considered for their design and for their effective integration within urban drainage systems. The analysis is structured around three main themes:

1. The effects of the storage volume on the outflow from the pond, a crucial aspect for verifying compliance with hydraulic invariance requirements and, more broadly, for managing discharges toward the receiving system;
2. The role of infiltration through the bottom of the pond, which significantly contributes to the overall hydrological efficiency of the system by reducing outflow volumes and enhancing the aquifer recharge (hydrological invariance);
3. The analysis of wet–dry cycles, which affects the functionality of the pond area, particularly when it serves multiple uses, and determines maintenance needs concerning, for instance, biological clogging or potential mosquito proliferation.

Two scenarios will be considered: (i) Scenario A, which includes two small ponds (pond W and pond E), each with a surface area of 100 m^2 and a depth of 1 m, and (ii) Scenario B, where the ponds are sized in accordance with the Italian hydraulic invariance regulations. In this case, the planimetric extensions are substantially larger, equal to 460 m^2 for pond W and 420 m^2 for pond E, while the height is set at 1 m. To complement the main discussion, additional analyses are presented to investigate the effects of seasonality on the internal hydrological processes. These evaluations make it possible to understand how climatic variability, precipitation patterns, and evapotranspiration influence the system efficiency and the behavior of the ponds throughout the year.

The main characteristics of the two systems are reported in Table 1. As shown in the table, the western area (system W) has a larger contributing area compared to eastern one (system E); however, this difference becomes less pronounced when considering the runoff volumes generated by the two drainage areas due to the significant contrast in their runoff coefficients. Peak flows in the two systems depend not only on the contributing areas and their runoff potential but also on the aggregation effects introduced by the conduit network. The E system is relatively longer than the W system, mainly due to the need to collect and separate first-flush runoff. It is also important to note that the use of a 30-year rainfall record provides a statistically robust set of results, allowing the analysis to move beyond the common design assumption of a return period between rainfall and discharge. The latter assumption is often not valid in real hydrological systems, where strong non-linearities shape the rainfall/runoff transformation.

Table 1. Characteristics of the catchment and of the infiltration ponds.

	West System	**East System**
Total surface	15,054 m^2	6853 m^2
Impervious surface fraction	0.46	1
Pervious surface fraction	0.54	0
Prescribed storage volume	460 m^3	450 m^3
Pond surface (Scenario A)	100 m^2	100 m^2
Pond surface (Scenario B)	460 m^2	450 m^2
Pond maximum level	1 m	1 m
Soil thickness layer	4 m	4 m
Porosity	0.35	0.35
Saturated conductivity	36 mm/h	36 mm/h
Suction head	150 mm	150 mm

Using a single 30-year rainfall record does not allow reliable extrapolation to return periods beyond the observed range thus, results should be interpreted within the return period domain typically considered in urban drainage system design. However, targeting extreme events would require complementary stochastic approaches for the generation of synthetic time series of hydrological variables, introducing additional methodological complexity and uncertainty; for this reason, we relied on the available observed record.

The proposed approach relies on metrics primarily focused on the quantitative and operational/maintenance performance of the pond and does not explicitly address water quality issues, either in terms of pollutant load reduction within the pond or in terms of potential risks to the underlying aquifer. Both aspects are highly site-specific, depending on local regulatory thresholds, so results are not readily generalizable.

Figure 3 depicts, for both the W and E systems, the return periods T_R associated with the annual maximum inflow Q_{in} (blue markers) and the corresponding outflow Q_{out} from the pond. Red markers represent Scenario A, while orange markers represent Scenario B. The two panels refer to the W system and the E system, respectively. Return periods were derived using the Weibull formula for empirical frequencies:

$$F(Q_i) = \frac{i}{N+1} \qquad T_R(Q_i) = \frac{1}{1 - F(Q_i)} \tag{1}$$

with Q_i as the sorted discharge. Focusing on a specific scenario, a similar behavior can be observed for both systems. In Scenario A (red markers), the effect of the small pond is visible through the peak discharge attenuation ($Q_{out,i} < Q_{in,i}$), which leads to an increase in the return period ($T_R(Q_{out}) > T_R(Q_{in})$). However, in this scenario, the attenuation capacity is limited by the small storage volume selected. The pond has some impact on smaller return periods (i.e., inflows with $T_R < 10$ years), whereas its effect becomes marginal for the larger observed peaks. This behavior is expected, as the highest inflow values typically occur when the pond is already full, an occurrence that may happen frequently for the small pond in scenario A.

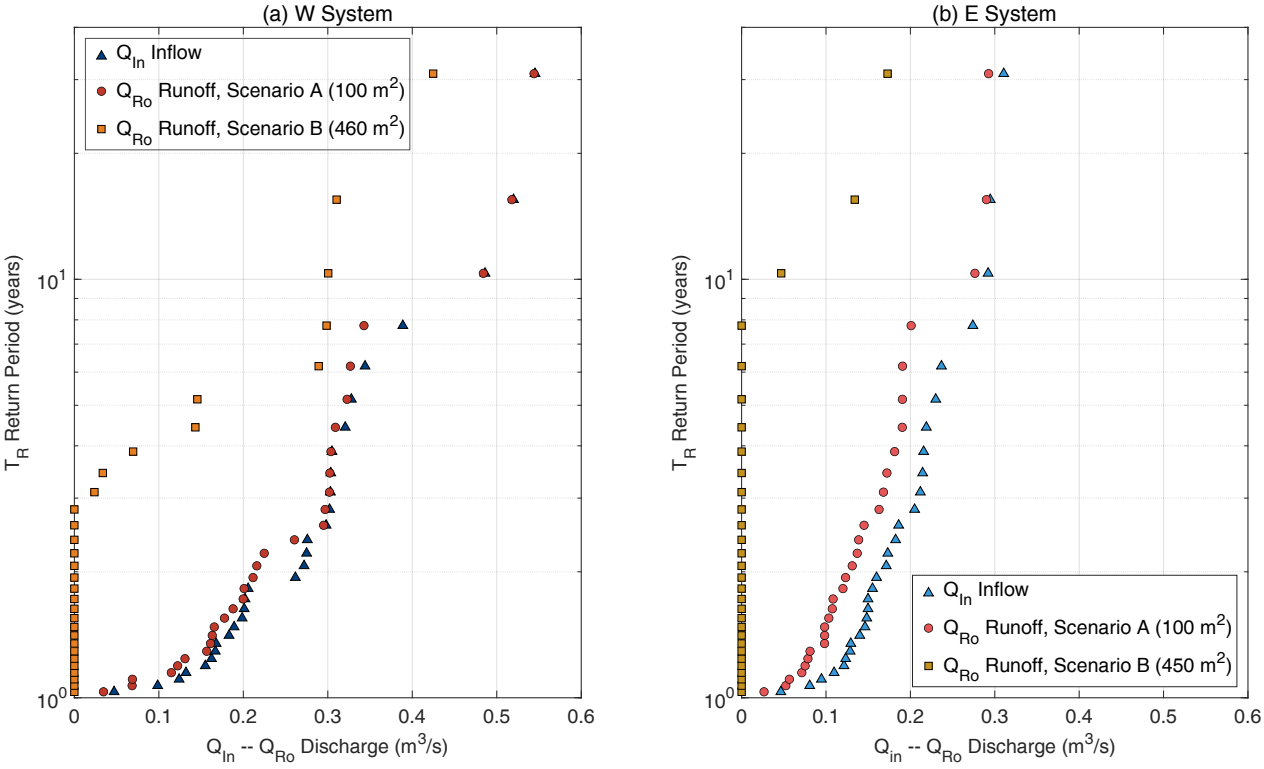

Figure 3. Return periods of the annual maximum inflow Q_{in} (blue) and the corresponding outflow Q_{rn} discharged by the pond for scenario A (red) and Scenario B (orange). Panels (**a**,**b**) refer to the W system and the E system.

A completely different behavior emerges in Scenario B, where the presence of the two large storage volumes produces a substantial attenuation of peak flows and a marked shift in return periods, which increase from approximately 2 years up to nearly 10 years

depending on the discharge value. Moreover, in more than half of the simulated events, the outflow from the ponds drops to zero, indicating that the available storage is sufficient to fully retain ordinary inflow volumes without releasing any discharge to the downstream system. It is important to emphasize that, under Scenario B, the hydraulic effect of the ponds becomes essentially equivalent to that of conventional grey stormwater detention tanks, with a strong regulation of outflows and a substantial reduction of peak values. The slightly stronger attenuation observed for pond E can be attributed to its more extensive drainage network, which induces a more pronounced phase shift between incoming and aggregated hydrographs, thus further reducing peak discharges.

The considerations above must be interpreted in light of the different design purposes of small-scale ponds. These systems are not primarily intended to attenuate annual maximum peak flows but rather to provide storage and promote infiltration or reuse under ordinary hydrological conditions. Consequently, the limited performance observed in Scenario A with respect to annual maxima, especially those associated with higher return periods, is consistent with expectations, whereas the strong attenuation observed in Scenario B reflects the much larger storage volumes adopted.

We now move to the analysis of water volumes, which represents a central aspect of this work. Figure 4 shows, using different colors for systems and scenarios, the time series of the cumulative volumes W_i of all the relevant hydrological variables, namely inflow, infiltration, recharge, evaporation, and runoff; the series includes the 30-year simulation period.

Focusing on Figure 4a, which corresponds to the small pond (Scenario A) serving the W system, it can be observed that infiltration (orange line) represents a substantial fraction of the inflow volume (blue line), while the remaining part is transformed almost entirely into runoff (red line); evaporation (cyan line) is negligible. Furthermore, nearly all the infiltrated water is transmitted downward as groundwater recharge (green line). A similar behavior is observed for pond E under the same scenario, as shown in Figure 4b.

We define the *hydrological efficiency* (η) of the pond as the ratio between the recharged volume (W_{rec}) and the inflow volume (W_{in})

$$\eta = \frac{W_{rec}}{W_{in}} \tag{2}$$

Here, η is a pond-specific metric and should be interpreted as an inflow to recharge efficiency conditional on the actual water delivered to the pond, i.e., the water available for infiltration after runoff-generation processes and the occurrence of hydrological losses in the subcatchments. We note that even in Scenario A, despite the small pond size, the long-term efficiency is remarkably high, $\eta = 0.73$ and $\eta = 0.79$ for the two systems, respectively.Figure 4c,d, corresponding to Scenario B, illustrate the behavior of the larger ponds. In this case, a slightly different pattern emerges: both ponds exhibit higher infiltration and recharge rates, with $\eta = 0.88$ and $\eta = 90$. Those high efficiency highlights the importance of the pond bottom area, since the infiltrated volume depends linearly on it. The larger storage capacity also acts as an additional driver of system efficiency.

In this second scenario, the most significant losses are associated with evaporation (from both the pond surface and the soil), which is also approximately proportional to the pond area. However, under a Mediterranean climate regime, precipitation and temperature, the two main drivers of infiltration and evapotranspiration, exhibit a favorable asynchrony: rainfall peaks in winter when temperatures and evaporation are at their minimum, and vice versa. This seasonal decoupling contributes to maximizing the infiltrated volume while minimizing evaporative losses. Nonetheless, even a small pond can play

a fundamental role in closing the local hydrologic cycle by functionally and efficiently reintroducing water into the subsurface.

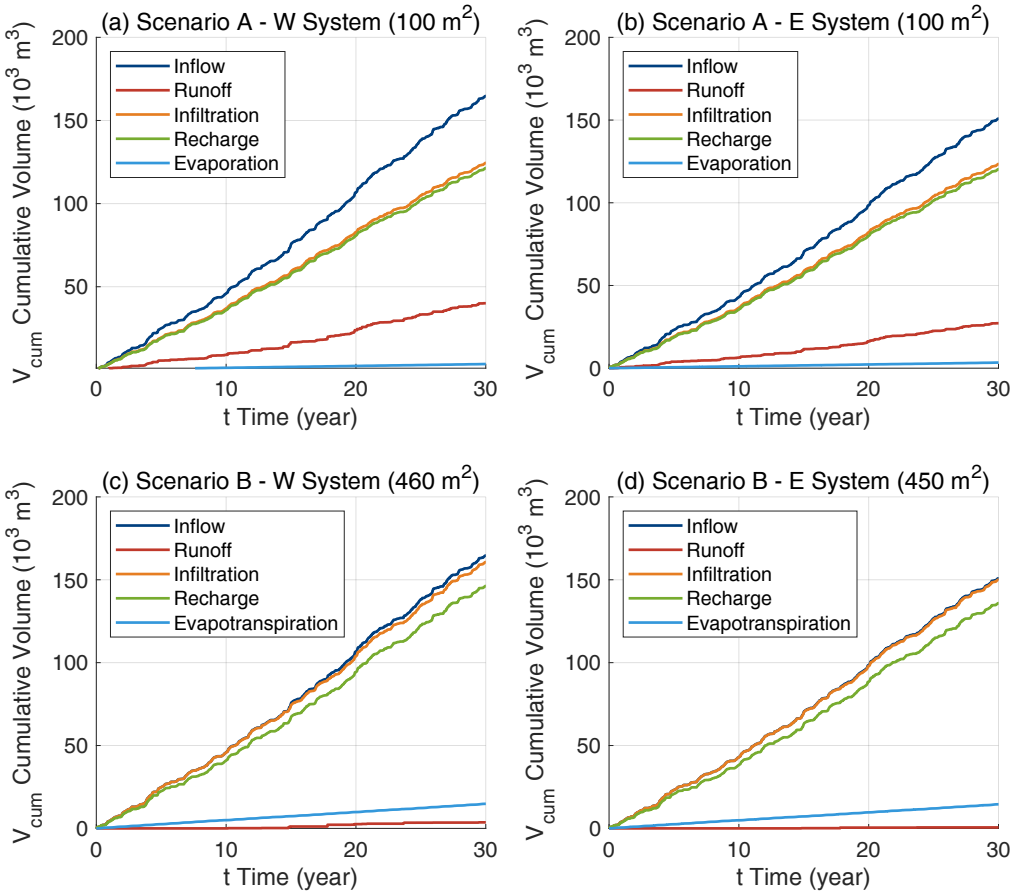

Figure 4. Cumulative time series of the main hydrological variables governing pond behavior, including inflow, runoff, infiltration, recharge, and evaporation. The different panels correspond to distinct systems and modeling scenarios.

The efficiency analysis is further explored in Figure 5, which shows the annual series of η (computed on a yearly basis) together with the annual precipitation. Years with the lowest efficiency (2008, 2011, 2017) occur under both above- and below-average rainfall, indicating that annual rainfall alone does not control efficiency. This erratic behavior can be attributed to the intra-annual distribution of rainfall. Although wetter years tend to trigger runoff more frequently (which represents the main loss in Scenario A), a key factor is the temporal structure of precipitation and the recurrence of closely spaced events. For small ponds, short, low-intensity, and frequent storms enhance infiltration and increase η, whereas concentrated events with large volumes markedly reduce efficiency.

For larger ponds (Scenario B, green and red markers), which generally achieve higher efficiencies, the lower η values are associated with the occasional activation of runoff (see Figure 3), while as long as the pond can contain incoming volumes, η remains high. Also, in this case, intra-annual variability still plays a role, but with a significant difference: larger surfaces induce higher evaporative losses than in Scenario A; under a Mediterranean climate, however, the seasonal decoupling between rainfall peaks (winter) and temperature/ET peaks (summer) mitigates the annual impact of evaporation, supporting long-term infiltration efficiency. The relationship between annual precipitation and efficiency η exhibits a scale-dependent behavior. Smaller ponds show a moderate negative correlation (approximately $\rho \simeq -0.4$ in both cases), which is primarily attributed to hydraulic limitations: during wetter years, the limited storage volume often leads to overflow, reducing the

fraction of infiltrated water. In contrast, larger pond sizes are characterized by a positive correlation ($\rho \simeq 0.4$–0.7), driven by increased infiltration capacity associated with higher soil moisture levels. Overall, the analysis suggests a useful (albeit context-dependent) design implication: in arid climates characterized by pronounced summer rainfall, storage in small ponds may be a highly efficient solution, as it reduces exposure to evaporation. Finally, we emphasize that pond efficiency η reflects performance as a function of the incoming precipitation volume, whereas the actually infiltrated volume remains strongly linked to the prevailing rainfall regime.

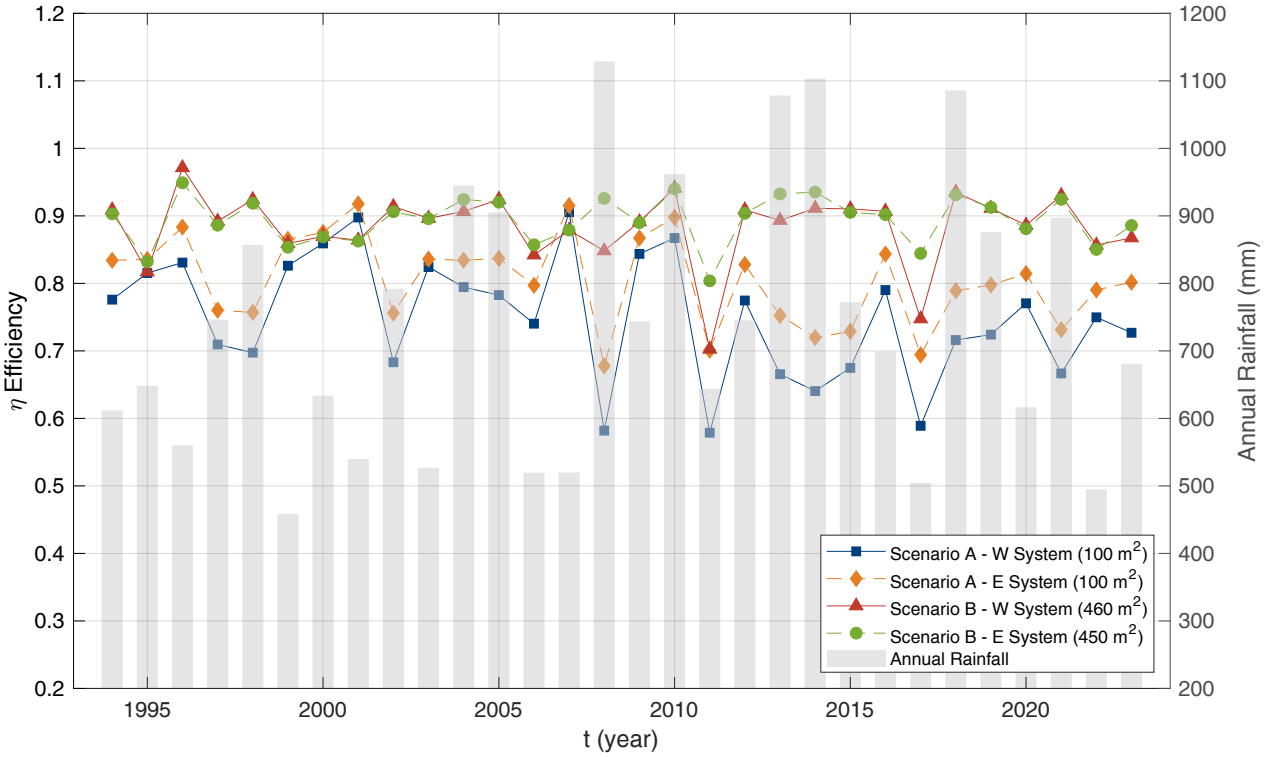

Figure 5. Time series of annual efficiency values (η). Different marker colors refer to the four cases analyzed, while grey bars indicate annual rainfall on the secondary (right) y-axis.

To complement the pond efficiency analysis, Figure 6 reports the monthly means μ_V of the inflow volume, the recharge volume, and the runoff volume. The analysis is presented for the W system only; the two panels refer to the two scenarios (Scenario A and Scenario B), while the E system is omitted because it exhibits a similar behavior. As observed in the inter-annual analysis, discussed in the previous paragraph, a strong correlation emerges between the recharge volume and the inflow: the months that maximize infiltration coincide with autumn–winter, when precipitation input is larger and the atmospheric energy balance reduces evaporative losses.

The comparison between Scenario A (small pond) and Scenario B (large pond) provides additional information: in the colder and wetter months, the larger storage capacity of Scenario B leads to a substantial reduction in runoff and, under lower temperatures, limits evaporative losses, resulting in higher infiltrated volumes. Conversely, during summer, deep infiltration is similar in the two scenarios. This is because the additional water stored in the larger pond is counterbalanced by increased evaporative losses.

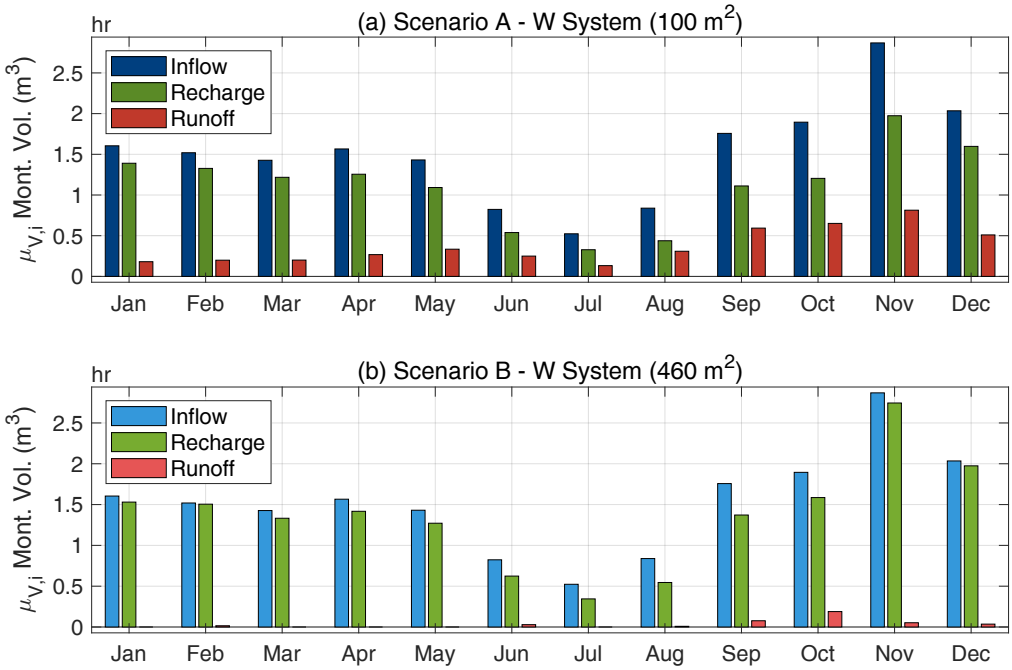

Figure 6. Monthly averages of volumes (μ_V) for inflow, recharge, and runoff for system W (1994–2023). Panel (**a**) refers to Scenario A (pond base area: 100 m^2), while Panel (**b**) refers to Scenario B (pond base area: 460 m^2).

The final analysis shifts the focus from hydrological efficiency to the temporal dynamics of the filling and emptying cycles, an aspect that is crucial for hydraulic functionality, which requires rapid recovery of available storage for the protection of the downstream receptor. Besides hydraulic functioning, the temporal cycle durations are crucial for pond management: they directly affect scheduled maintenance, such as the scraping of the clogged layer to restore infiltration capacity, as well as ecological implications, including soil oxygenation and mosquito control.

Figure 7 shows the frequency distributions $F(\delta)$ of dry and wet period durations δ observed over the entire simulation period (1994–2023). The two panels depict the distributions of dry and wet periods, respectively, while the curves within each panel compare systems (W, E) and scenarios (A, B).

In addition to their hydrological relevance, wet and dry cycles are also directly linked to pond operability and maintenance: prolonged wet conditions and repeated wetting may promote sediment deposition and surface sealing, potentially accelerating clogging, whereas sufficiently long dry windows provide the opportunity to carry out maintenance actions such as the scraping of the clogged surface layer aimed at restoring infiltration capacity.

In general, the frequencies of dry periods appear very similar in all cases, being largely governed by the precipitation pattern and, in particular, the sequence and inter-arrival time of rainfall events. We note a considerable variability in duration, spanning from very short periods to several tens of days. The distribution of wet-period durations (i.e., periods during which water is present in the pond) provides more informative insights. In this case, significant differences can be observed between the two scenarios. In Scenario B, the larger surface available for infiltration leads to faster emptying; this feature is particularly significant for ordinary events that are fully contained within the pond. For a given inflow volume, in larger ponds, water spreads over a wider area with lower water depths, which shortens the time required for drainage. In any case, whatever the scenario, the range of durations is quite small at a few days, much smaller than the dry periods; in fact, the duration of wet periods is strongly influenced by the volume of the pond

and its infiltration capacity. The simulation results show that the smaller ponds infiltrate the stored stormwater in less than two days in approximately 95% of cases, while the larger pond restores full functionality within two days in almost all occurrences. From a hydraulic perspective, these fast drawdown times support the use of the pond as a storage facility for hydraulic invariance and are consistent with widely adopted best practices of design, which typically target drawdown times of about 48–72 h, depending on particular regional guidelines.

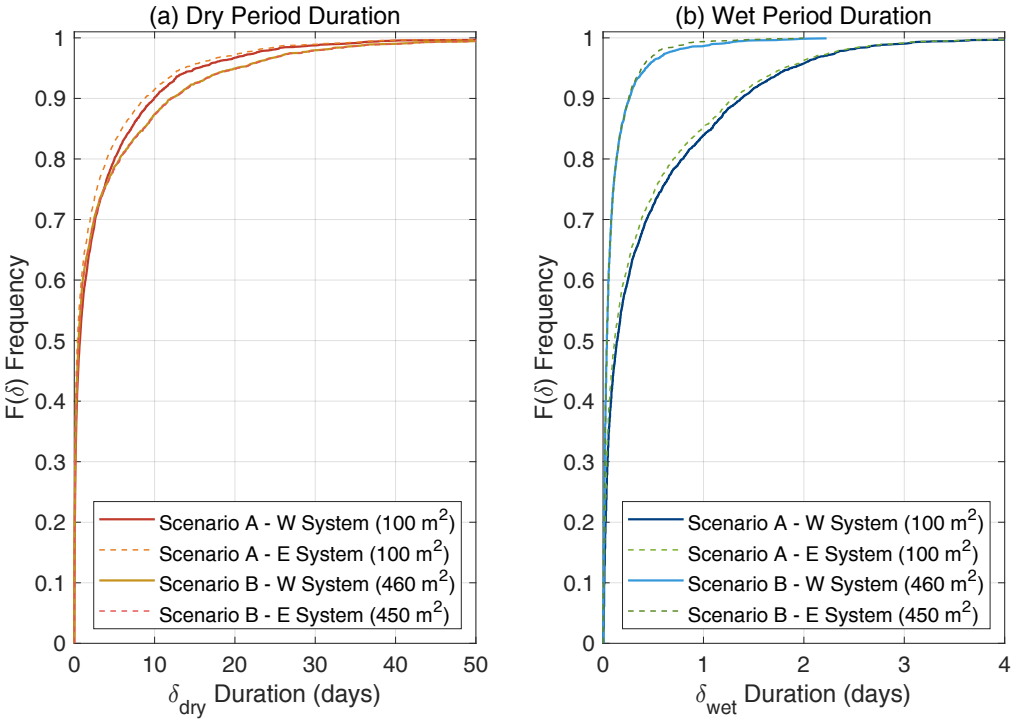

Figure 7. Frequency distributions of dry- and wet-period durations δ_i for the pond over 1994–2023. Panel (**a**) refers to dry periods, while Panel (**b**) refers to wet periods. Different colors and styles are associated with the different cases analyzed.

5. Conclusions

This study proposed a performance-based framework for the design and long-term assessment of infiltration ponds integrated within hybrid grey–green urban drainage systems. By combining detailed modeling of the grey network with multi-decadal continuous simulations of infiltration facilities, the approach overcomes key limitations of traditional event-based design and enables an explicit evaluation of hydraulic regulation, infiltration efficiency, and operational reliability under realistic climatic forcing. The Rome Technopole case study demonstrated how such a framework can support informed planning and design decisions in contexts where infiltration-based solutions are desirable but technical and regulatory guidance remains fragmented.

The results indicate that pond geometry, in particular bottom area and available storage, is the primary control on long-term system performance. Larger ponds can provide peak-flow attenuation comparable to conventional detention structures while simultaneously promoting high levels of infiltration and groundwater recharge, thereby supporting both hydraulic safety and the sustainable use of local water resources. Smaller ponds, despite their limited storage, still deliver substantial infiltration benefits under ordinary hydrological conditions, confirming their role as effective complementary components within integrated grey–green systems.

From a broader perspective, the analysis highlights the contribution of infiltration ponds to the sustainability of urban water management. By enhancing on-site water retention, reducing downstream discharges, and promoting groundwater recharge, these systems support a shift from purely conveyance-based drainage toward more resilient and resource-efficient urban water cycles. Continuous simulations further showed how climate seasonality modulates system performance, with Mediterranean conditions favoring infiltration efficiency by limiting evaporative losses during periods of high inflow. Beyond hydraulic and volumetric metrics, the explicit assessment of wet–dry cycles demonstrated that properly designed ponds may consistently restore their storage capacity within short timeframes. This behavior is essential not only for hydraulic functionality but also for long-term operational sustainability, as it underpins maintenance planning, ecological balance, and continued system effectiveness.

Overall, the main contribution of this work lies in providing a generalizable, practitioner-oriented methodology that links grey-system hydraulics with long-term LID performance assessment using widely available modeling tools. In the absence of harmonized design standards, the proposed framework offers a transparent and technically grounded basis to support the sustainable integration of nature-based solutions into urban drainage planning. Future research should extend this approach to synthetic rainfall and climate-change scenarios and explicitly incorporate water-quality and vadose-zone transport processes to further strengthen the role of infiltration-based systems in sustainable urban water management.

Author Contributions: Conceptualization, A.Z. and A.F.; methodology, A.Z. and A.F.; software, A.Z.; formal analysis, A.Z. and A.F.; data curation, A.Z.; writing—original draft preparation, A.Z.; writing—review and editing, A.F.; visualization, A.Z. All authors have read and agreed to the published version of the manuscript.

Funding: This research was funded by the Project "Ecosistema dell'innovazione—Rome Technopole" financed by EU-Next-GenerationEU, CUP:F83B22000040006.

Institutional Review Board Statement: Not applicable.

Informed Consent Statement: Not applicable.

Data Availability Statement: The SWMM models used in this study are publicly available on Zenodo at https://doi.org/10.5281/zenodo.19606749, accessed on 17 April 2026, including all input files and internal time series required to run the simulations.

Conflicts of Interest: The authors declare no conflicts of interest.

References

1. Miller , J.D.; Kim, H.; Kjeldsen, T.R.; Packman, J.; Grebby, S.; Dearden, R. Assessing the impact of urbanization on storm runoff in a peri-urban catchment using historical change in impervious cover. *J. Hydrol.* **2014**, *515*, 59–70. [CrossRef]
2. Narducci, P. *Sulla Fognatura Della Città di Roma: Descrizione Tecnica Dell'ingegnere Cav. Pietro Narducci*; Forzani E. C., Tipografi del Senato: Roma, Italy, 1889.
3. Bianchi, E. (Ed.) *La Cloaca Maxima e i Sistemi Fognari di Roma Dall'antichità ad Oggi*; Palombi Editori: Roma, Italy, 2014; Atti del Convegno, Istituto Nazionale di Studi Romani: Roma, Italy, 2012.
4. Sun, Y.; Deng, L.; Pan, S.Y.; Chiang, P.C.; Sable, S.S.; Shah, K.J. Integration of green and gray infrastructures for sponge city: Water and energy nexus. *Water-Energy Nexus* **2020**, *3*, 29–40. [CrossRef]
5. Lashford, C.; Rubinato, M.; Cai, Y.; Hou, J.; Abolfathi, S.; Coupe, S.; Charlesworth, S.; Tait, S. SuDS & Sponge Cities: A Comparative Analysis of the Implementation of Pluvial Flood Management in the UK and China. *Sustainability* **2019**, *11*, 213. [CrossRef]
6. Alves, A.; Gersonius, B.; Sanchez, A.; Vojinovic, Z.; Kapelan, Z. Multi-criteria Approach for Selection of Green and Grey Infrastructure to Reduce Flood Risk and Increase CO-benefits. *Water Resour. Manag.* **2018**, *32*, 7. [CrossRef]

7. de Macedo, M.B.; Júnior, M.N.G.; de Oliveira, T.R.P.; Giacomoni, M.H.; Imani, M.; Zhang, K.; do Lago, C.A.F.; Mendiondo, E.M. Low Impact Development practices in the context of United Nations Sustainable Development Goals: A new concept, lessons learned and challenges. *Crit. Rev. Environ. Sci. Technol.* **2022**, *52*, 2538–2581. [CrossRef]
8. Esraz-Ul-Zannat, M.; Dedekorkut-Howes, A.; Morgan, E.A. A review of nature-based infrastructures and their effectiveness for urban flood risk mitigation. *WIREs Clim. Change* **2024**, *15*, e889. [CrossRef]
9. Leng, L.; Jia, H.; Chen, A.S.; Zhu, D.Z.; Xu, T.; Yu, S. Multi-objective optimization for green-grey infrastructures in response to external uncertainties. *Sci. Total Environ.* **2021**, *775*, 145831. [CrossRef]
10. Voskamp, I.; Van de Ven, F. Planning support system for climate adaptation: Composing effective sets of blue-green measures to reduce urban vulnerability to extreme weather events. *Build. Environ.* **2015**, *83*, 159–167. [CrossRef]
11. Eckart, K.; McPhee, Z.; Bolisetti, T. Performance and implementation of low impact development—A review. *Sci. Total Environ.* **2017**, *607–608*, 413–432. [CrossRef]
12. Onuma, A.; Tsuge, T. Comparing green infrastructure as ecosystem-based disaster risk reduction with gray infrastructure in terms of costs and benefits under uncertainty: A theoretical approach. *Int. J. Disaster Risk Reduct.* **2018**, *32*, 22–28. [CrossRef]
13. Taylor, L.; Hochuli, D.F. Defining greenspace: Multiple uses across multiple disciplines. *Landsc. Urban Plan.* **2017**, *158*, 25–38. [CrossRef]
14. Lafortezza, R.; Davies, C.; Sanesi, G.; Konijnendijk, C. Green Infrastructure as a tool to support spatial planning in European urban regions. *IForest-Biogeosci. For.* **2013**, *6*, 102–108. [CrossRef]
15. Bouwer, H. Artificial recharge of groundwater: Hydrogeology and engineering. *Hydrogeol. J.* **2002**, *10*, 121–142. [CrossRef]
16. Newcomer, M.E.; Gurdak, J.J.; Sklar, L.S.; Nanus, L. Urban recharge beneath low impact development and effects of climate variability and change. *Water Resour. Res.* **2014**, *50*, 1716–1734. [CrossRef]
17. Scholz, M. (Ed.) Preface. In *Wetlands for Water Pollution Control*, 3rd ed.; Elsevier: Amsterdam, The Netherlands, 2024; pp. xxxiii–xxxvi. [CrossRef]
18. Rossman, L.A.; Huber, W.C. *Storm Water Management Model Reference Manual, Volume III: Water Quality*; EPA/600/R-16/093; U.S. Environmental Protection Agency: Cincinnati, OH, USA, 2016.
19. Washington State Department of Ecology. *Ecology BMP T7.10—Infiltration Basins*; Stormwater Management Manual for Western Washington; Washington State Department of Ecology: Olympia, WA, USA, 2019; Volume V.
20. CIRIA. *The SuDS Manual (C753)*; Construction Industry Research and Information Association: London, UK, 2015.
21. European Commission. *Infiltration Basins (U12): Natural Water Retention Measures*; European Commission: Brussels, Belgium, 2014.
22. Massmann, J. *A Design Manual for Sizing Infiltration Ponds*; Report No. WA-RD 578.2; Washington State Department of Transportation: Olympia, WA, USA, 2003.
23. California Department of Transportation. *Infiltration Basin Design Guide*; Caltrans, Division of Design: Sacramento, CA, USA, 2020.
24. Asry, A.; Lipeme Kouyi, G.; Fletcher, T.D.; Bonneau, J.; Tedoldi, D.; Lassabatere, L. Sets of infiltration models for water infiltration in sustainable urban drainage systems. *J. Hydrol.* **2023**, *623*, 129477. [CrossRef]
25. Job, C. A Review of Low-Impact Development Factors Affecting Managed Aquifer Recharge. *Groundwater* **2022**, *60*, 619–627. [CrossRef]
26. Riva, M.; Mambretti, S.; Chaynikov, S.; Ackerer, P.; Fasunwon, O.; Guadagnini, A. New General Analytical Solution for Infiltration Structures Design. *J. Hydraul. Eng.* **2013**, *139*, 637–644. [CrossRef]
27. Akan, A.O.; Houghtalen, R.J. *Urban Hydrology, Hydraulics, and Stormwater Quality: Engineering Applications and Computer Modeling*; John Wiley & Sons: Hoboken, NJ, USA, 2003.
28. Raimondi, A.; Becciu, G. On pre-filling probability of flood control detention facilities. *Urban Water J.* **2015**, *12*, 344–351. [CrossRef]
29. Stafford, N.; Che, D.; Mays, L.W. Optimization Model for the Design of Infiltration Basins. *Water Resour. Manag.* **2015**, *29*, 2789–2804. [CrossRef]
30. Nazari, A.; Roozbahani, A.; Hashemy Shahdany, S.M. Integrated SUSTAIN–SWMM–MCDM Approach for Optimal Selection of LID Practices in Urban Stormwater Systems. *Water Resour. Manag.* **2023**, *37*, 3769–3793. [CrossRef]
31. Ma, D.; Wu, S.; Liu, Z.; Zhang, J. A Novel Analytical Solution for Ponded Infiltration With Consideration of a Developing Saturated Zone. *Water Resour. Res.* **2023**, *59*, e2022WR034228. [CrossRef]
32. Motlagh, A. Urban Stormwater and Groundwater Quality: Pathways, Risks, and Green Infrastructure Solutions. *Environments* **2025**, *12*, 446. [CrossRef]
33. Tedoldi, D.; Couvidat, J.; Gautier, M.; Zhan, Q.; Winiarski, T.; Lipeme Kouyi, G.; Delolme, C.; Chatain, V. In-depth characterization of sediment contamination in stormwater infiltration basins. *Blue-Green Syst.* **2023**, *6*, 1–19. [CrossRef]
34. Fiori, A.; de Barros, F.P.; Bellin, A. An analytical framework for risk evaluation and design of infiltration basins for Managed Aquifer Recharge. *Water Resour. Res.* **2025**, *61*, e2024WR038516. [CrossRef]
35. Geberemariam, T.K. Finite difference method to design sustainable infiltration-based stormwater management system. *Int. J. Water Resour. Environ. Eng.* **2019**, *11*, 112–119. [CrossRef]

36. Moreno, Z.; Paster, A.; Kamai, T. A Wetting-Front Model for Vadose Zone Infiltration via Drywells. *Water Resour. Res.* **2023**, *59*, e2022WR033554. [CrossRef]
37. Fischer, S.; Dallan, E.; Fiori, A.; Grimaldi, S.; Kochanek, K.; Prieto, C.; Reis, D.S., Jr.; Volpi, E. Hydrological design in the HELPING decade–inspiring the community to innovate the hydrological design concept. *Hydrol. Sci. J.* **2025**, *70*, 375–389.
38. Liu, T.; Lawluvy, Y.; Shi, Y.; Yap, P.S. Low Impact Development (LID) Practices: A Review on Recent Developments, Challenges and Prospects. *Water Air Soil Pollut.* **2021**, *232*, 344. [CrossRef]
39. Li, Q.; Wang, F.; Yu, Y.; Huang, Z.; Li, M.; Guan, Y. Comprehensive performance evaluation of LID practices for the sponge city construction: A case study in Guangxi, China. *J. Environ. Manag.* **2019**, *231*, 10–20. [CrossRef]
40. Grimaldi, S.; Petroselli, A.; Serinaldi, F. Design hydrograph estimation in small and ungauged watersheds: Continuous simulation method versus event-based approach. *Hydrol. Process.* **2012**, *26*, 3124–3134. [CrossRef]
41. Cipollini, S.; Fiori, A.; Volpi, E. Structure-based framework for the design and risk assessment of hydraulic structures, with application to offline flood detention basins. *J. Hydrol.* **2021**, *600*, 126527. [CrossRef]
42. Fiori, A.; Mancini, C.; Annis, A.; Lollai, S.; Volpi, E.; Nardi, F.; Grimaldi, S. The role of residual risk on flood damage assessment: A continuous hydrologic-hydraulic modelling approach for the historical city of Rome, Italy. *J. Hydrol. Reg. Stud.* **2023**, *49*, 101506. [CrossRef]
43. Cappelli, F.; Volpi, E.; Langousis, A.; Deidda, R.; Perdios, A.; Furcolo, P.; Grimaldi, S. Sub-daily rainfall simulation using multifractal canonical disaggregation: A parsimonious calibration strategy based on intensity-duration-frequency curves. *Stoch. Environ. Res. Risk Assess.* **2025**, *39*, 1–19. [CrossRef]
44. Rossman, L.A. *Storm Water Management Model User's Manual Version 5.1*; National Risk Management Research Laboratory, Office of Research and Development, US Environmental Protection Agency: Washington, DC, USA, 2017.
45. Vigna, F.L.; Mazza, R.; Amanti, M.; Salvo, C.D.; Petitta, M.; Pizzino, L.; Pietrosante, A.; Martarelli, L.; Bonfà, I.; Capelli, G.; et al. Groundwater of Rome. *J. Maps* **2016**, *12*, 88–93. [CrossRef]
46. Macro, K.; Matott, L.S.; Rabideau, A.; Ghodsi, S.H.; Zhu, Z. OSTRICH-SWMM: A new multi-objective optimization tool for green infrastructure planning with SWMM. *Environ. Model. Softw.* **2019**, *113*, 42–47. [CrossRef]
47. Luan, B.; Yin, R.; Xu, P.; Wang, X.; Yang, X.; Zhang, L.; Tang, X. Evaluating Green Stormwater Infrastructure strategies efficiencies in a rapidly urbanizing catchment using SWMM-based TOPSIS. *J. Clean. Prod.* **2019**, *223*, 680–691. [CrossRef]
48. Liao, Z.L.; Zhang, G.Q.; Wu, Z.H.; He, Y.; Chen, H. Combined sewer overflow control with LID based on SWMM: An example in Shanghai, China. *Water Sci. Technol.* **2015**, *71*, 1136–1142. [CrossRef]
49. Hargreaves, G.H.; Allen, R.G. History and Evaluation of Hargreaves Evapotranspiration Equation. *J. Irrig. Drain. Eng.* **2003**, *129*, 53–63. [CrossRef]
50. Hargreaves, G.H.; Samani, Z.A. Reference Crop Evapotranspiration from Temperature. *Appl. Eng. Agric.* **1985**, *1*, 96–99. [CrossRef]
51. Moeletsi, M.E.; Walker, S.; Hamandawana, H. Comparison of the Hargreaves and Samani Equation and the Thornthwaite Equation for Estimating Dekadal Evapotranspiration in the Free State Province, South Africa. *Phys. Chem. Earth Parts A/B/C* **2013**, *66*, 4–15. [CrossRef]
52. Sparks, A.H. nasapower: A NASA POWER Global Meteorology, Surface Solar Energy and Climatology Data Client for R. *J. Open Source Softw.* **2018**, *3*, 1035. [CrossRef]